

Bandwidth Considerations for Multilevel Converters

Geoff Walker, *Member, IEEE*, and Gerard Ledwich, *Senior Member, IEEE*

Abstract—Multilevel converters can achieve an overall effective switch frequency multiplication and consequent ripple reduction through the cancellation of the lowest order switch frequency terms. This paper investigates the harmonic content and the frequency response of these multimodulator converters. It is shown that the transfer function of uniformly sampled modulators is a Bessel function associated with the inherent sampling process. Naturally sampled modulators have a flat transfer function, but multiple switchings per switch cycle will occur unless the input is slew-rate limited.

Lower sideband harmonics of the effective carrier frequency and, in uniform converters, harmonics of the input signal also limit the useful bandwidth. Observations about the effect of the number of converters, their type (naturally or uniformly sampled), and the ratio of modulating frequency and switch frequency are made.

Index Terms—Natural PWM, modulation, multilevel converters, uniform PWM.

I. MULTILEVEL CONVERTERS

A MULTILEVEL converter has a multiple of the usual six switches found in a three-phase inverter. The main motivation for such converters is that voltage [in a voltage-source inverter (VSI) and current in a current-source inverter (CSI)] is shared among these multiple switches, allowing a higher converter power rating than the individual switch volt-ampere (VA) rating would otherwise allow. This sharing is achieved by summing the outputs of several two-level converters with transformers or inductors [1], or direct series connection, or by more complex topologies such as the diode-clamped inverter and the flying capacitor inverter [2], [3]. An example of a multilevel flying capacitor voltage source converter is shown in Fig. 1.

Another secondary, but very important advantage is the extra degrees of switching freedom that the multiple switches permit. Each switch still has the same limited switching frequency, but by staggering the switching instants of the individual switches, the overall switching frequency of the multilevel converter effectively becomes a multiple of that of the individual switches [1]. A further gain comes since we switch between *multiple* voltage levels at this higher frequency rather than two, so the switching harmonics appear at a higher frequency *and* a lower level (see Fig. 2). Overall converter input and output ripple is much reduced, and less filtering is required. This is an important advantage in a high-power

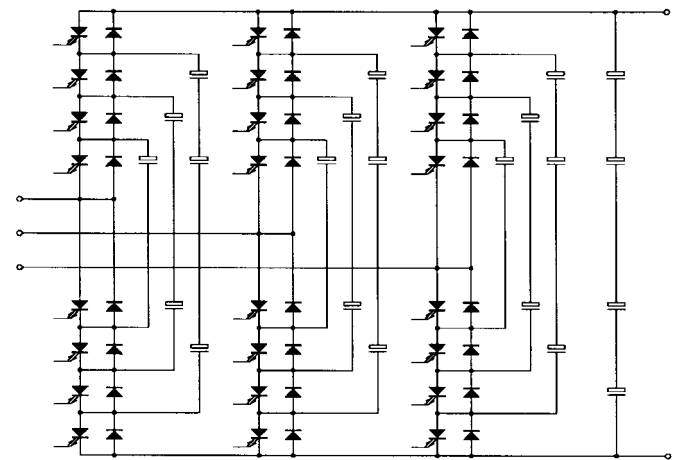


Fig. 1. An example of a multilevel converter—a five-level (nine-level phase-phase) flying capacitor converter [3].

converter where the switching frequency is low and filtering is expensive.

Many different approaches to multilevel control have been published. The diode-clamped topology imposes restrictions on allowed switch states and requires further control to maintain the auxiliary capacitors at their correct voltages. As a consequence, the control and modulation of these converters are treated as one whole problem. Extensions of subharmonic and precalculated optimized [4], space voltage vector [5], and hysteresis [6] control strategies have all been made.

A more modular control scheme is usually adopted for flying capacitor and multibridge converters [1], [8].

This paper only examines naturally and uniformly sampled synchronous pulsewidth modulation (SPWM), as these techniques are easily implemented, produce good results for moderate switch frequencies, and are easily extended to multibridge converters. In particular, the bandwidth and harmonics of these two techniques are examined, both for single and multimodulator converters.

In any case, space-vector modulation and uniform sampled PWM have been shown to be closely related [7]. Space-vector modulation does uniformly sample the input, and the following results for uniformly sampled PWM apply equally to space-vector modulation.

II. THEORY

A. Naturally Sampled PWM

In naturally sampled PWM (natural PWM), the switching instants are generated by the intersection of a triangle carrier wave with the input waveform (see Fig. 3). The input waveform is *naturally sampled* by the carrier wave; the sampling

Manuscript received May 5, 1997; revised May 14, 1998. Recommended by Associate Editor, T. Habetler.

G. Walker is with the Department of Computer Science and Electrical Engineering, University of Queensland, St. Lucia, Australia.

G. Ledwich is with the Department of Electrical Engineering, University of Newcastle, Australia.

Publisher Item Identifier S 0885-8993(99)00288-4.

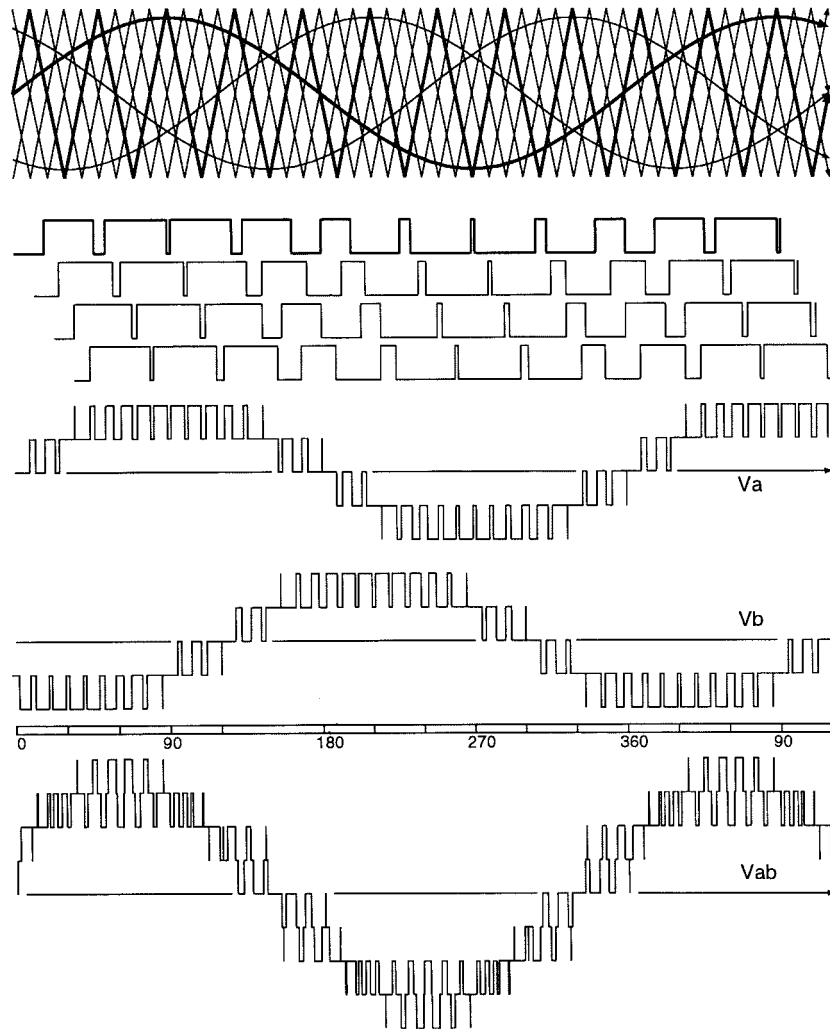


Fig. 2. Three-phase synchronous carrier PWM, $N = 9$, and $M = 0.9$. From the top, the three sine waves of frequency f_1 intersect with four triangular carriers of frequency f_c to produce 12 PWM waveforms. The four PWM control waveforms associated with phase A are shown and then the resultant five-level phase A PWM waveform when these are added as a result of the structure of the converter. The five-level phase B waveform is similarly produced, and the nine-level phase-phase waveform is the difference of these.

instant occurring at the same instant as the output edge. SPWM occurs when the carrier or switch frequency f_c is a multiple of the input signal's frequency f_1 and is the usual practice for a low-pulse number $N = f_c/f_1$.

For natural SPWM, the spectrum consists of the input signal f_1 , the carrier and its harmonics mf_c , and their associated sidebands $mf_c \pm nf_1$ (see Fig. 6). The amplitudes of these spectral terms are given by Bessel functions and are a function of modulation depth M (the amplitude of the modulating signal f_1) as well as frequency.

No harmonics or intermodulation products of the input signal are generated. The frequency response of the modulator itself is flat. The overall response of the converter is determined only by the output filter (see Figs. 4, 5, and 7).

A limit is, however, imposed on the input signal's slew rate if multiple switching edges per switch cycle are to be avoided. The slope of the input signal should not exceed the slope of the triangular carrier wave by remaining within the boundary $Mf_1 < 2/\pi f_c$.

It should be noted that a limit on input signal's slew rate does not limit the bandwidth as such, but rather the

available bandwidth at a given amplitude. If higher frequency components in the input signal occur at lower amplitudes—as is often the case in active filters—then these can be reproduced without attenuation and without violating the slew-rate limit. Furthermore, if multiple switching edges and the resultant rise in switch frequency can be tolerated, then high-frequency input signals will continue to be faithfully synthesized, without distortion or intermodulation products.

The natural PWM modulator is quite simply implemented in analog hardware, but does not lend itself to microcontroller implementation as the switching instants are defined by transcendental equations. Being analog, untrimmed accuracy of the triangular carrier's amplitude, and thus switching instants, is limited to $\pm 5\%$. This leads to poor cancellation of spectral terms in multilevel converters, and even after trimming, the analog-generated natural PWM still cannot match the digitally implemented uniform PWM in this area.

B. Uniformly Sampled PWM

In uniformly or regularly sampled PWM (uniform PWM), the input signal is regularly sampled at the beginning of

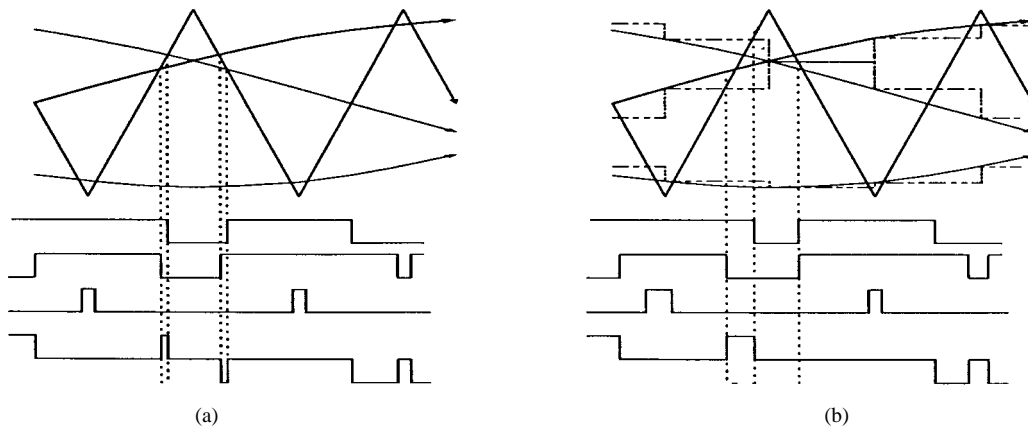


Fig. 3. The process of (a) natural and (b) uniform sampling. Uniform sampling introduces a delay of on average $T_{\text{sam}}/2$ which causes a sinc-like frequency response.

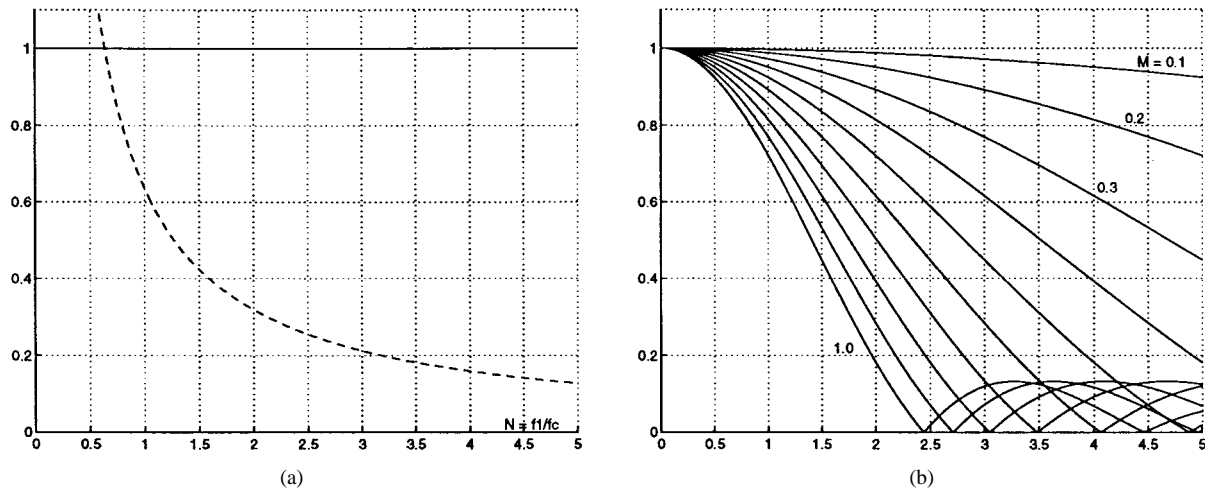


Fig. 4. The transfer function (versus the ratio f_1/f_c) of (a) natural and (b) uniform PWM modulators. Natural modulation introduces no attenuation or phase delay, but is subject to a slew-rate limit (dotted) if multiple pulses per switch cycle are to be avoided. For uniform modulation, the attenuation is a function of both modulation depth M and the ratio of modulating signal frequency to carrier (switch) frequency (f_1/f_c).

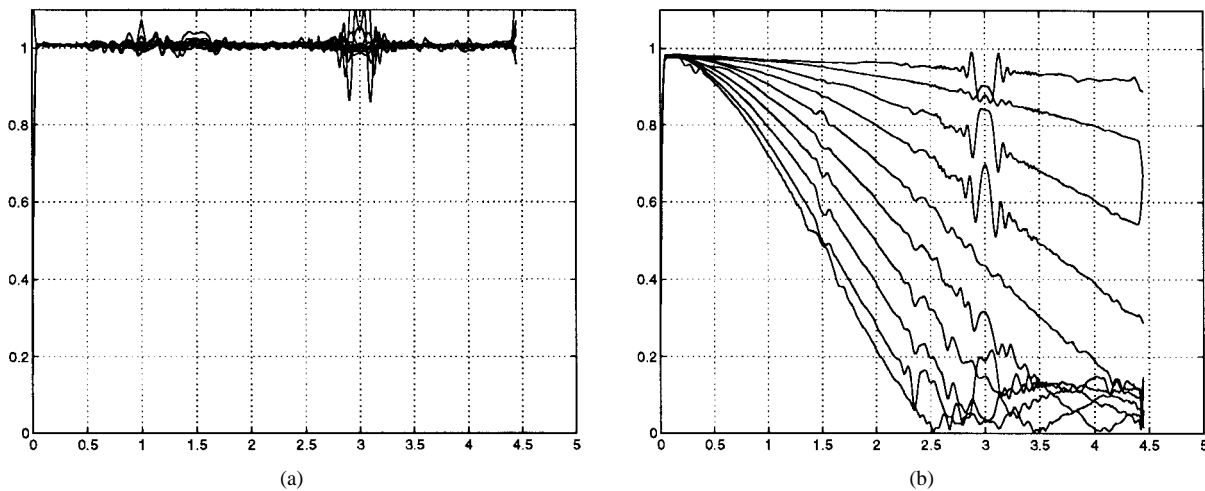


Fig. 5. The measured transfer function (for f_1/f_c) of (a) natural and (b) uniform PWM modulators is in clear agreement with theory.

each switch cycle before being compared with the triangle waveform. While this complicates an analog implementation, this approach is easily implemented with a microcontroller. The resultant spectrum of the output resembles natural PWM, however, harmonics of the input signal $n f_1$ exist, and the input

signal is attenuated at higher frequencies (see Figs. 4, 5, and 8).

The PWM output spectra of natural (1) and uniform (2) double-edge synchronous modulation are represented in Fig. 6 as the sum of their constituent harmonics [9].

$$V_{nat}(m, n) = e^{j\Phi_1} e^{j2\pi f_1 t} + \sum_{m, n | (m+n) \text{ odd}, m \neq 0} \frac{J_n(M\frac{\pi}{2}m)}{\pi m} e^{j(n\Phi_1 - m\Phi_c)} e^{j2\pi(mf_c + nf_1)t} \quad (1)$$

$$V_{uni}(m, n) = \sum_{m, n | (m+n) \text{ odd}} \frac{J_n(M\frac{\pi}{2}(m + nf_1/f_c))}{\pi(m + nf_1/f_c)} e^{j(n\Phi_1 - m\Phi_c - \frac{\pi}{2}(m + nf_1/f_c))} e^{j2\pi(mf_c + nf_1)t} \quad (2)$$

where f_1 input signal frequency Φ_1 input signal phase, $(0 \dots 2\pi)$
 f_c carrier (switch) frequency Φ_c carrier phase, $(0 \dots 2\pi)$
 m, n integers, such that ... $mf_c + nf_1$ output frequency spectral terms
 M modulation depth. $(0 \dots 1)$

Fig. 6. The frequency spectra of natural and uniform sampled double-edge PWM for a sine-wave input of frequency f_1 .

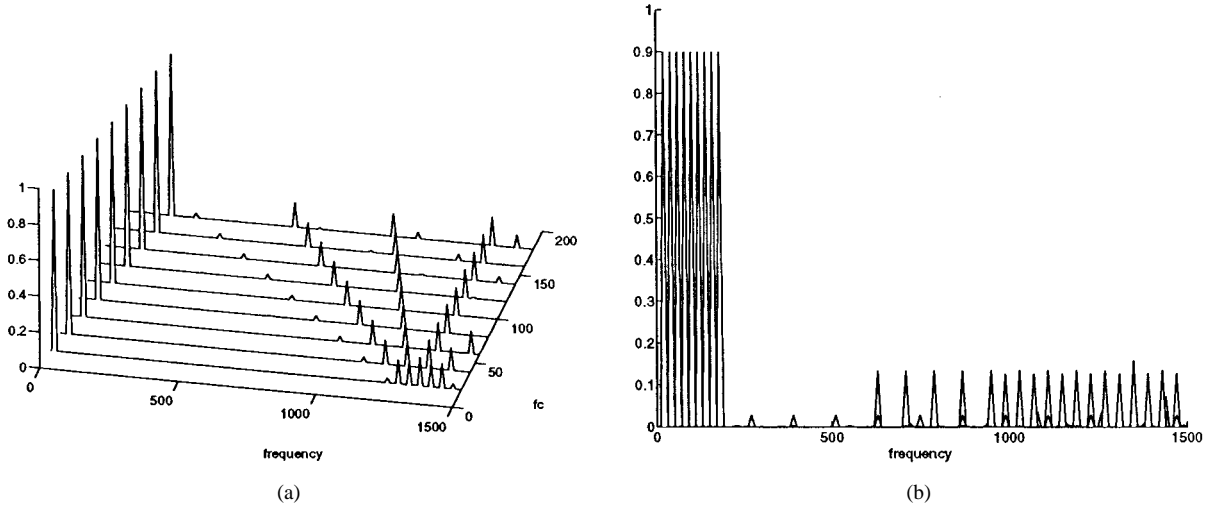


Fig. 7. This waterfall plot and its front elevation show the spectra of a naturally sampled four-level converter for different input frequencies. $M = 0.9$ and $f_c = 450$ Hz.

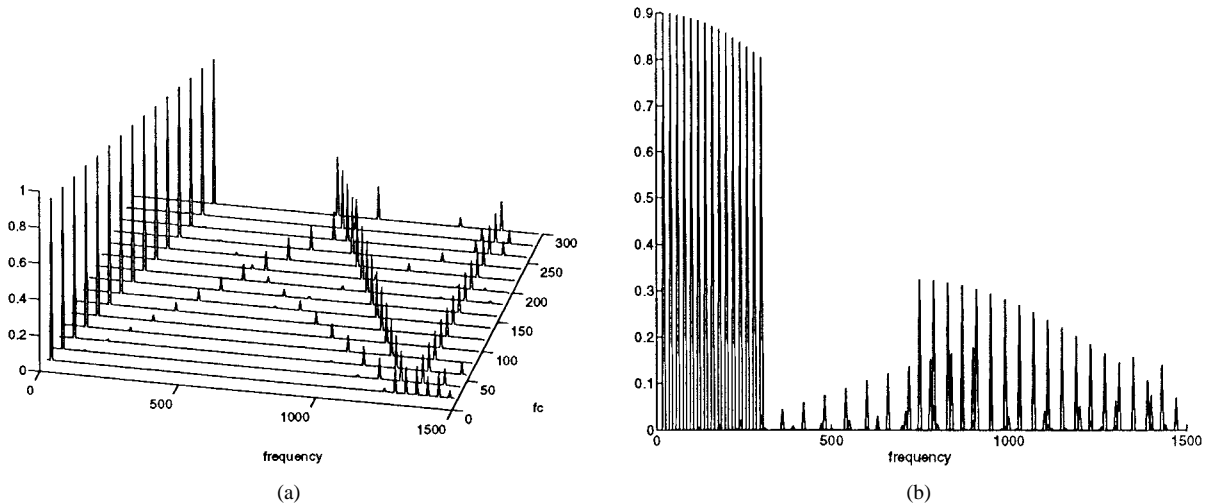


Fig. 8. This waterfall plot and its front elevation show the spectra of a uniformly sampled four-level converter for different input frequencies. Note that the input signal response is not flat and the presence of input signal harmonics [cf. natural sampling (see Fig. 7)] $M = 0.9$ and $f_c = 450$ Hz.

Usually, the ratio f_1/f_c is large, in which case uniform PWM is very similar in performance to natural PWM. As the input frequency rises and, thus, this ratio falls, the input signal response rolls off and the amplitude of both input signal harmonics and sideband harmonics increases (see Fig. 8). This may limit the use of uniform sampling with a low-carrier frequency.

C. Extension to Multiple Modulators

Referring to (1) and (2), the phase of the input signal term ($m = 0, n = 1$) in natural PWM remains equal to Φ_1 , but in uniform PWM, some phase shift is introduced by the sampling process $\Phi_1 - \pi/2f_1/f_c$. This delay can become significant as the ratio f_1/f_c increases and should be considered in wide-

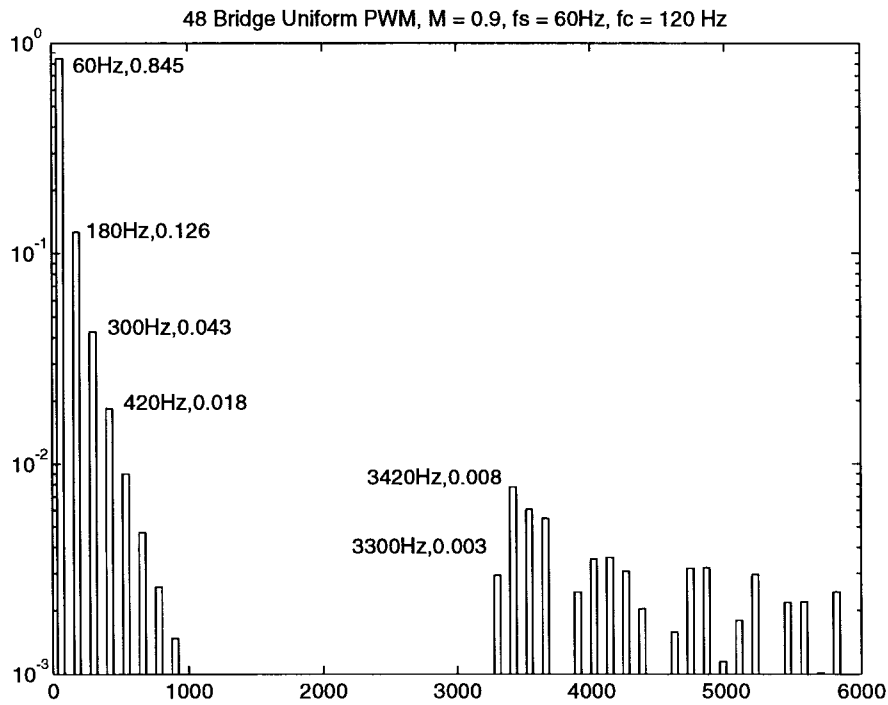


Fig. 9. The hypothetical consequence of using uniform sampling for a 49-level converter when $N = f_c/f_1 = 2$. The synthesized fundamental has been attenuated, and odd harmonic distortion overwhelms the switch frequency terms.

bandwidth closed-loop stability calculations. For both natural and uniform PWM, changing the carrier phase Φ_c does not affect the phase of the input signal term, as $m = 0$, but does affect the carrier and its sidebands, as $m \neq 0$. In multimodulator converters, choosing Φ_{ci} for each modulator such that $\sum m\Phi_{ci} = 0$ will cancel all carrier and sidebands of order m . As an example, the simulations and practical results in this paper apply to a three-bridge four-level converter. Each bridge carrier was phase shifted by $2\pi/3$ so although the switch frequency $f_c = 450$ Hz, only spectral components associated with $m = 0, 3, 6, \dots$ appear in the PWM output.

This result opens up the possibility of using a large number of low-frequency bridges in high-power applications (for example, 48 modules with 120-Hz carrier frequency [8]), however, difficulties arise in practice which theory and ideal simulations might not predict (see Section IV).

III. RESULTS

A number of Matlab routines (".m" files) have been written to calculate and display the spectral components generated by single and multiple converters, both natural and uniform sampled. The switching instants of the edges are calculated directly for the uniformly sampled case and iteratively for the naturally sampled case. Nonideal effects such as time quantization, switching delays, and dead times can also be easily included at this point. Jump function analysis [10] is then used to calculate the exact Fourier spectrum of these PWM waveforms and avoids the problems of the fast Fourier transform (FFT). These files have proved to be useful tools for the prediction of spectra.

A four-level naturally sampled modulator was built in hardware. Three triangle reference waves were generated by

integrating square waves, and then these were compared with the modulating wave to generate the PWM signals. These three PWM signals were summed to give a four-level output waveform. Stable and accurate phase-shifted clock signals were provided by an 80C196 microcontroller rather than discrete logic for simplicity and flexibility.

A four-level uniformly sampled modulator based entirely on an 80C196 was also developed. The internal 10-b analog-digital (A-D) converter samples the modulating waveform before every edge. This value is scaled and becomes a time offset which is added to the mean switching instant. At this calculated time, one of three output pins is set or cleared appropriately by the high-speed-output peripheral.

The spectral results of the two hardware approaches were collected and calculated with a dedicated spectrum analyzer—the Tektronics 2630. This spectral data was imported into Matlab and plotted along with the predicted values for comparison. In the figures, the measured data appears as a continuous (1024 pt) spectrum, with spikes peaking (hopefully) at the predicted values indicated by horizontal bars.

IV. DISCUSSION OF RESULTS

The relative performance of the different modulators (natural versus uniform and analog versus digital) is compared under a number of headings: carrier cancellation, signal distortion, and interference by the lower sidebands.

A. Carrier Cancellation

In a multilevel converter, cancellation of suppressed carriers and their sidebands should be complete, and this was seen

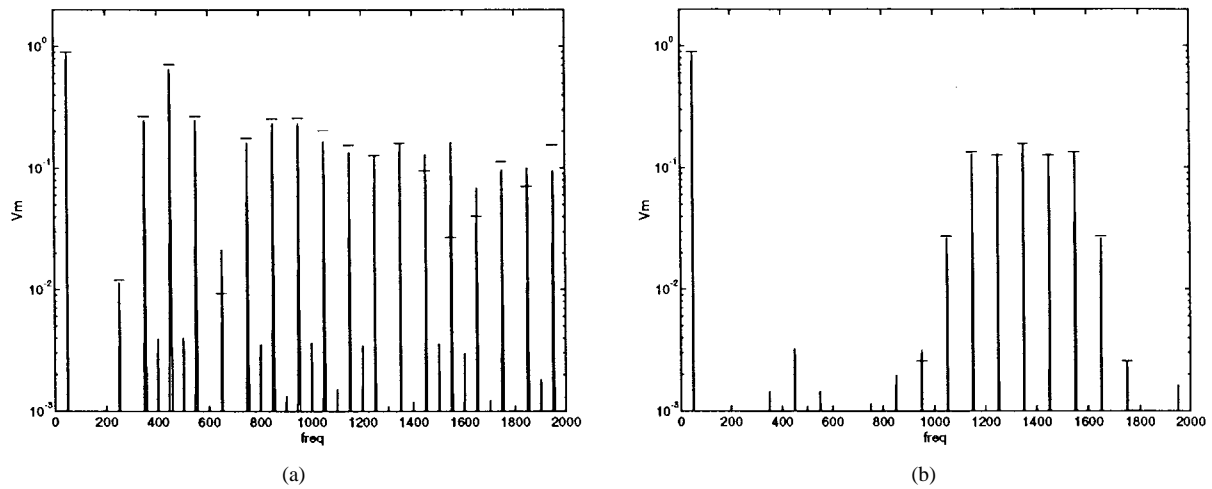


Fig. 10. These spectra compare the predicted and measured spectra of (a) naturally sampled two- and (b) four-level converters. $M = 0.9$ and $N = 9$ ($f_1 = 50$ Hz and $f_c = 450$ Hz).

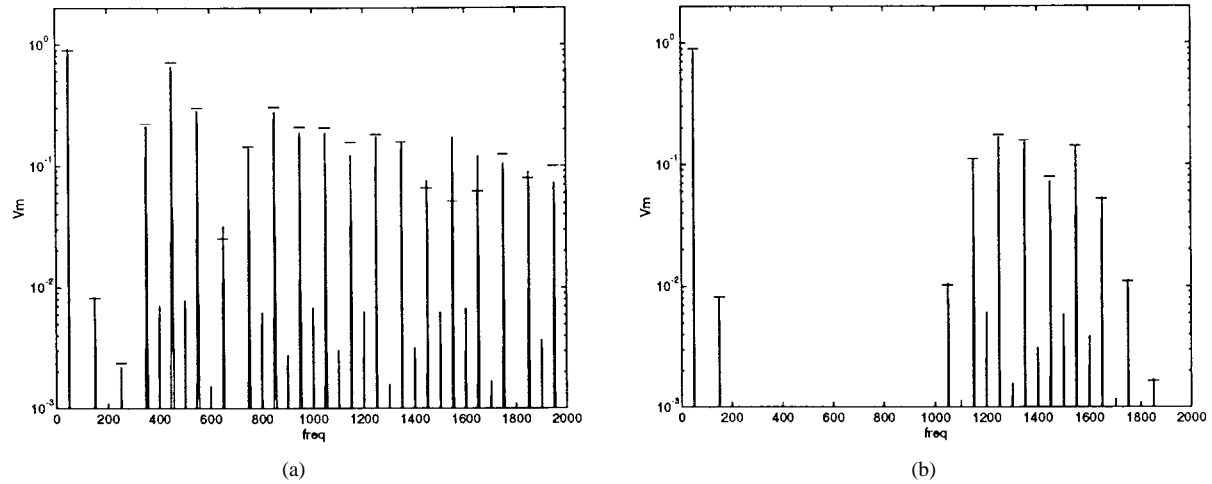


Fig. 11. These two spectra compare the predicted and measured spectra of (a) uniformly sampled two- and (b) four-level converters. $M = 0.9$ and $N = 9$ ($f_1 = 50$ Hz and $f_c = 450$ Hz).

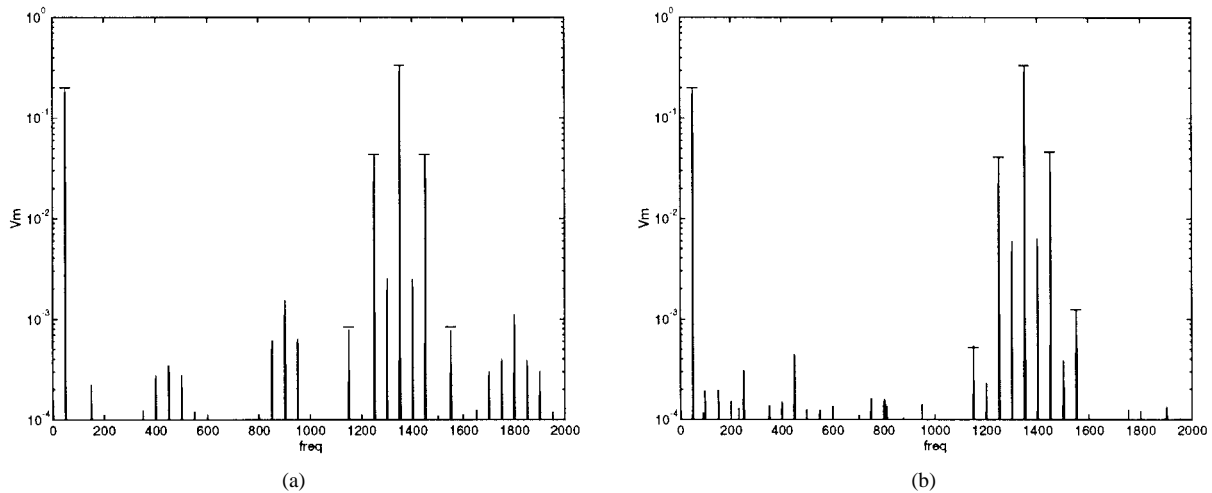


Fig. 12. These two spectra compare the predicted and measured spectra of (a) naturally and (b) uniformly sampled four-level converters at low-modulation depth. $M = 0.2$ and $N = 9$ ($f_1 = 50$ Hz and $f_c = 450$ Hz).

in the simulations. In practice, inaccuracies in the generation of switching instants from bridge to bridge will lead to poor cancellation of harmonic terms. The uniform sampled

converter did achieve excellent cancellation, with only the 450-Hz carrier ($V_m \approx 3e-4$) visible above the noise floor ($V_m \leq 1e-4$) (see Fig. 11). This is due to the precision of the digital

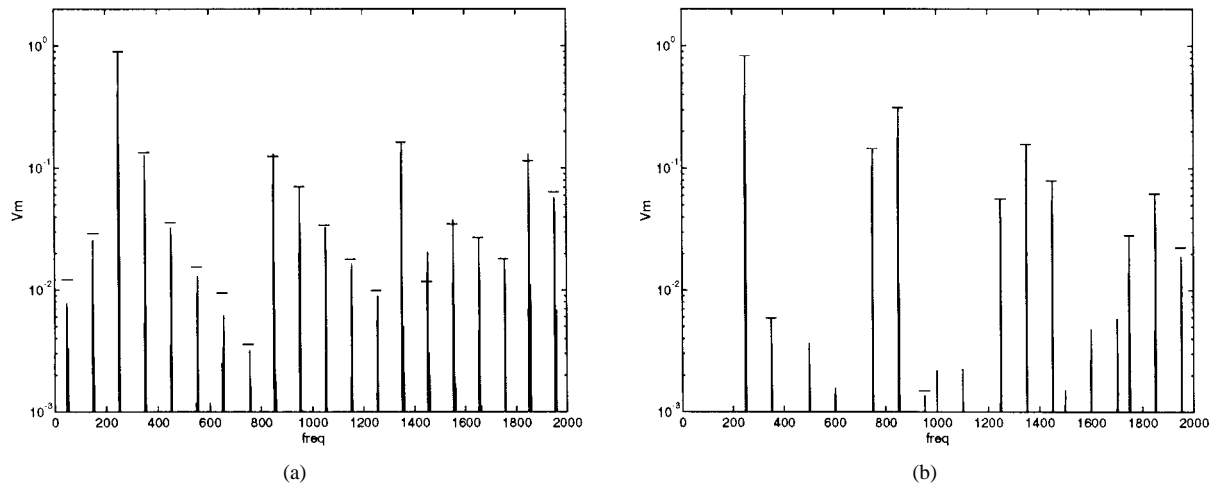


Fig. 13. These two spectra compare the predicted and measured spectra of (a) naturally and (b) uniformly sampled four-level converters at a higher input frequency. $M = 0.9$ and $N = 1.8$ ($f_1 = 250$ Hz and $f_c = 450$ Hz).

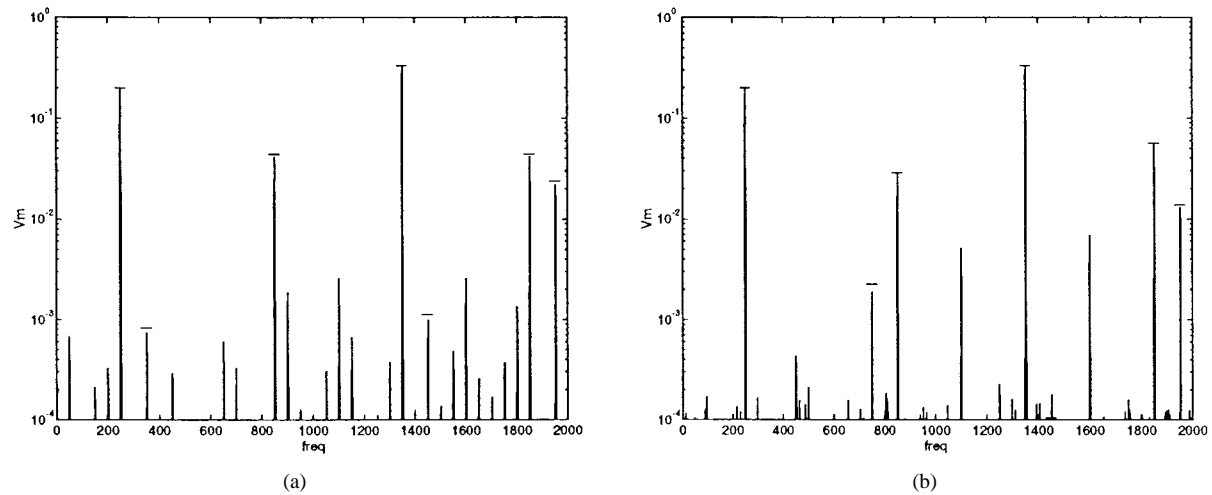


Fig. 14. These two spectra compare the predicted and measured spectra of (a) naturally and (b) uniformly sampled four-level converters at a higher input frequency, but a low-modulation depth. $M = 0.2$ and $N = 1.8$ ($f_1 = 250$ Hz and $f_c = 450$ Hz).

implementation of the uniform converter and not attributable to the uniform sampling process itself.

The natural converter did not achieve the same order of cancellation ($V_m \approx 3e-3$ at 450 Hz and $M = 0.9$) (see Fig. 10). This is simply because of the analog nature of the circuitry and the consequent inequalities between each of the three modulators. The results shown were achieved after trimming the amplitudes of each integrator, as standard tolerance components led to poor cancellation. In terms of precision, the digital modulator has a distinct advantage over the analog modulator.

B. Harmonic Distortion

In theory, the naturally sampled PWM does not generate any harmonics of the input signal, however, some low-level distortion terms are visible in practice (e.g., for 50 Hz, $M = 0.9$ and the 150-Hz third harmonic $\approx 6e-4$). This is in contrast to uniform PWM which does generate harmonics of the fundamental (e.g., as above, but uniform $\approx 8e-3$).

Although these distortion components are small in these measurements, they do become the limiting factor in some

larger systems. To illustrate this problem, a 48 modulator system was simulated using uniform sampling. The amplitude of the harmonic distortion components can be seen to overwhelm the switch frequency spectral terms (Fig. 9). Some researchers advancing the cause of multilevel FACTS converters have recognized the need for modulators with a linear transfer function [11], such as the sine-triangle natural sampled modulator.

At low-modulation depths, natural and uniform modulators are very similar spectrally, and uniform sampling is relatively distortion free (Fig. 12). In the limit as the signal amplitude goes to zero, the only difference is that of a pure delay of half of a switch subcycle.

C. Carrier Spectral Interference

The lower sideband harmonics of the carrier remain constant in amplitude for a natural sampled modulator, as can be seen in the waterfall plot (see Fig. 7), while those of a uniform modulator oscillate, eventually dying away. For this reason, uniform sampling does appear to have an advantage for higher

frequency modulating signals of large amplitude (Fig. 13). This advantage disappears at lower amplitudes (Fig. 14).

For large systems with many modulators, the first significant sidebands usually meet the input signal when $f_1/f_c = 1$ and so limit the large-signal bandwidth to this value (see Figs. 7 and 8).

In summary, good carrier cancellation can be achieved with digitally generated uniform PWM, which would suggest the feasibility of low-carrier frequencies and multiple bridges in high-power applications. However, low-carrier frequencies lead to a large ratio of f_1/f_c and the associated problems of fundamental input signal attenuation, phase lag, and significant odd harmonic distortion. Multiple modulator converters cannot hide these problems. Furthermore, when time quantization was included in the simulations, little impact was made on the spectra for the three-modulator system, but as the number of modulators rose, so did the impact of time quantization on distortion terms and previously cancelled carrier terms.

V. CONCLUSION

Multimodulator converters can achieve an effective increase in overall switch frequency through the cancellation of the lowest order switch frequency terms. This paper has examined natural and uniform PWM modulation techniques to determine if this allows a similar effective bandwidth increase. The PWM output spectra were calculated mathematically, simulated using Matlab, collected from hardware implementations of the modulators, and the results evaluated and compared.

Naturally sampled PWM does not attenuate the synthesized fundamental nor generate any distortion products of the fundamental, so it appears more promising in theory. In practice, as the number of converters increases, the variation between the analog-generated carriers makes it increasingly difficult to achieve good carrier cancellation. The digitally generated uniform PWM can achieve consistently good cancellation of carrier terms. However, uniform PWM attenuates the input signal and generates input signal harmonics, with these effects becoming more pronounced as the ratio f_1/f_c rises. This limits uniform PWM's usefulness in low-pulse-number applications.

Lower sideband harmonics of the first nonzero carrier can also limit the large-signal bandwidth of both techniques. The first significant harmonics generally meet the input signal when $f_1/f_c = 1$, however, their amplitude decreases as the number of converters increases.

REFERENCES

- [1] K. Matsui, Y. Murai, M. Watanabe, M. Kaneko, and F. Ueda, "A pulsewidth modulated inverter with parallel connected transistors using

current-sharing reactors," *IEEE Trans. Power Electron.*, vol. 8, pp. 186–191, Apr. 1993.

- [2] F. Z. Peng and J. S. Lai, "Multilevel converters—A new breed of power converters," *IEEE Trans. Ind. Applicat.*, vol. 32, pp. 509–517, May/June 1996.
- [3] T. Meynard and H. Foch, "Multi-level conversion: High voltage choppers and voltage source inverters," in *IEEE Power Electronics Specialists Conf. (PESC)*, 1992, pp. 397–403.
- [4] B. Velaerts, P. Mathys, E. Tatakis, and G. Bingen, "A novel approach to the generation of an optimization of three-level PWM waveforms," in *IEEE Power Electronics Specialists Conf. (PESC)*, 1988, pp. 1255–1262.
- [5] M. Koyama, T. Fujii, R. Uchida, and T. Kawabata, "Space voltage vector-based new PWM method for large capacity three-level GTO inverter," in *IECON '92*, vol. 1, pp. 271–276.
- [6] M. Maresoni, "High performance current control techniques for applications to multilevel high-power voltage source inverters," *IEEE Trans. Power Electron.*, vol. 7, pp. 189–204, Jan. 1992.
- [7] D. G. Holmes, "The general relationship between regular-sampled pulse-width-modulation and space vector modulation for hard switched converters," in *IEEE Ind. Applicat. Meet.*, 1992, pp. 1002–1009.
- [8] Z. Zhang and B. Ooi, "Multimodular current source SPWM converters for a superconducting magnetic energy storage system," *IEEE Trans. Power Electron.*, vol. 8, pp. 250–256, July 1993.
- [9] P. Wolfs and G. Ledwich, "New methods of spectral analysis for pulse width modulators," in *ISSPA '87*, Aug. 1987, pp. 897–902.
- [10] P. Biringer and M. Slonim, "Determination of harmonics of converter current and/or voltage waveforms (new method for Fourier coefficient calculations), Part I: Fourier coefficients of homogeneous functions," *IEEE Trans. Ind. Applicat.*, vol. IA-16, pp. 242–247, Mar./Apr. 1980.
- [11] B. Mwinyiwiwa, Z. Wolanski, and B. Ooi, "High power switch mode linear amplifiers for flexible ac transmission system," *IEEE Trans. Power Delivery*, vol. 11, pp. 1993–1998, Oct. 1996.



Geoff Walker (M'98) was born in Brisbane, Australia, in 1969. He received the B.E. degree from the University of Queensland, St. Lucia, Australia, in 1990. He is currently working toward the Ph.D. degree in power electronics at the University of Queensland.

He has worked in both the professional audio and industrial electronics industries, performing both design and repair work. Most recently, he was with Baltec Systems, an electrostatic precipitator controller manufacturer. He is currently a Lecturer in the Department of Computer Science and Electrical Engineering, University of Queensland. His interests are in the areas of power electronics, industrial electronics, electric machines, and digital signal processing.

Gerard Ledwich (M'73–SM'92) was born in Melbourne, Australia, in 1951. He received the B.E. degree from the University of Queensland, St. Lucia, Australia, in 1972 and the Ph.D. degree from the University of Newcastle, Australia, in 1976.

He was with the University of Queensland and the Queensland Electricity Commission. He has been a Visiting Professor at different universities. He is currently the Pacific Power Professor of Power Engineering at the University of Newcastle. His research interests include power system analyses, power electronics, and control systems.

Dr. Ledwich is a Fellow of the Institution of Engineers, Australia.